Dickkopf-1 (DKK-1) Stimulated Prostate Cancer Growth and Metastasis and Inhibited Bone Formation in Osteoblastic Bone Metastases

Nanda K. Thudi,[1] Chelsea K. Martin,[2] Sridhar Murahari,[3] Sherry T. Shu,[2] Lisa G. Lanigan,[2] Jillian L. Werbeck,[2] Evan T. Keller,[4] Laurie K. McCauley,[5] Joseph J. Pinzone,[6] and Thomas J. Rosol[2]*

[1]*M.D. Anderson Cancer Center, University of Texas, Houston, Texas*
[2]*Department of Veterinary Biosciences, The Ohio State University, Columbus, Ohio*
[3]*Department of Veterinary Clinical Sciences, The Ohio State University, Columbus, Ohio*
[4]*Departments of Urology and Pathology, School of Medicine, University of Michigan, Ann Arbor, Michigan*
[5]*Department of Periodontics and Oral Medicine, School of Dentistry, University of Michigan, Ann Arbor, Michigan*
[6]*Department of Internal Medicine, The Ohio State University, Columbus, Ohio*

BACKGROUND. Osteoblastic bone metastasis is the predominant phenotype observed in prostate cancer patients and is associated with high patient mortality and morbidity. However, the mechanisms determining the development of this phenotype are not well understood. Prostate cancer cells secrete several osteogenic factors including Wnt proteins, which are not only osteoinductive but also oncogenic. Therefore, the purpose of the study was to investigate the contribution of the Wnt signaling pathway in prostate cancer growth, incidence of bone metastases, and osteoblastic phenotype of bone metastases. The strategy involved overexpressing the Wnt antagonist, DKK-1, in the mixed osteoblastic and osteolytic Ace-1 prostate cancer cells.
METHODS. Ace-1 prostate cancer cells stably expressing human DKK-1 or empty vector were established and transduced with lentiviral yellow fluorescent protein (YFP)-luciferase (Luc). The Ace-1/vector$^{YFP\text{-}LUC}$ and Ace-1/DKK-1$^{YFP\text{-}LUC}$ cells were injected subcutaneously, intratibially, or in the left cardiac ventricle in athymic mice.
RESULTS. Unexpectedly, DKK-1 significantly increased Ace-1 subcutaneous tumor mass and the incidence of bone metastases after intracardiac injection of Ace-1 cells. DKK-1 increased Ace-1 tumor growth associated with increased phospho46 c-Jun amino-terminal kinase by the Wnt noncanonical pathway. As expected, DKK-1 decreased the Ace-1 osteoblastic phenotype of bone metastases, as confirmed by radiographic, histopathologic, and microcomputed tomographic analysis. DKK-1 decreased osteoblastic activity via the Wnt canonical pathway evidenced by an inhibition of T-cell factor activity in murine osteoblast precursor ST2 cells.
CONCLUSION. The present study showed that DKK-1 is a potent inhibitor of bone growth in prostate cancer-induced osteoblastic metastases. *Prostate 71: 615–625, 2011.*

KEY WORDS: **prostate cancer; DKK-1; metastasis**

INTRODUCTION

Prostate cancer patients frequently develop bone metastases in late stages of the disease [1]. Most of the bone metastases are osteoblastic resulting in excessive, but poor quality, bone formation [2,3]. Osteoblastic metastases result in spinal cord compression, pathologic fractures, and pain resulting in severe morbidity of patients [4]. Using the Ace-1 model we previously showed that prostate cancer directly induced new bone

Grant sponsor: National Cancer Institute; Grant number: 2P01 CA93900; Grant sponsor: The Ohio State University College of Veterinary Medicine; Grant number: 520026.

Joseph J. Pinzone's present address is Amgen, Thousand Oaks, CA 91320.

*Correspondence to: Thomas J. Rosol, DVM, PhD, 1925 Coffey Road, Columbus, OH 43210. E-mail: rosol.1@osu.edu
Received 19 May 2010; Accepted 24 August 2010
DOI 10.1002/pros.21277
Published online 18 October 2010 in Wiley Online Library (wileyonlinelibrary.com).

formation in athymic mice [5,6]. Mechanisms responsible for prostate cancer osteoblastic bone metastases are not clearly defined [7].

Prostate cancer produces Wnt proteins, which were shown to possess tumorigenic and osteogenic potential [8]. Wnts are a large family of soluble proteins that contribute to normal development and embryogenesis [9]. However, dysregulated Wnt signaling has been implicated in the development of multiple cancer types, including prostate cancer [10]. Additionally, several Wnts were reported to be upregulated in cancers resulting in increased growth [11–13]. Wnts act through both canonical and noncanonical pathways [14].

The canonical Wnt pathway acts by binding to low density lipoprotein receptor proteins (LRP) and frizzled receptors on target cells to induce Wnt signaling [15]. Wnt signaling dissociates the β-catenin destruction complex consisting of axin, adenomatous polyposis coli (APC), and glycogen synthase kinase 3β (GSK3β), which leads to phosphorylation of β-catenin for ubiquitination and proteosomal degradation in the cytoplasm [8]. Therefore, in the presence of Wnts, β-catenin is stabilized and translocated into the nucleus where it binds to, and activates, T-cell factor (TCF). TCF acts on downstream target genes that are important for cell survival, proliferation, and angiogenesis [16]. Consequently, upregulation of the Wnt signaling pathway was shown to promote tumor survival and progression [17].

Wnts are important for the development and maintenance of bone by inducing the differentiation and maturation of precursor osteoblasts to active osteoblasts [18]. Secretion of Wnts in prostate cancer was also shown to play an important role in the development of osteoblastic metastases [19]. Dickkopf-1 (DKK-1) antagonizes Wnts by binding to the LRP receptor on the target cells, resulting in internalization of the receptor and inhibition of Wnt-mediated canonical signaling [15]. DKK-1 has been reported to be downregulated in prostate cancer patients in advanced stages [20]. Moreover, DKK-1 was overexpressed in breast cancer patients who develop predominantly osteolytic bone metastases [15,21].

Therefore, the hypothesis for this study was that inhibition of Wnt signaling by DKK-1 will decrease both prostate cancer growth in an autocrine manner and prostate cancer-induced osteoblastic metastases in a paracrine manner. To test this hypothesis, Ace-1 prostate cancer cells that develop mixed osteoblastic and osteolytic bone metastases were transfected to overexpress DKK-1. In this study, the functional role of overexpression of DKK-1 on prostate cancer growth, incidence of bone metastases, and osteoblastic phenotype of bone metastases was investigated.

MATERIALS AND METHODS

Cell Culture

The canine Ace-1 prostate cancer cells (derived from a spontaneous dog prostate carcinoma by our laboratory) [22] were maintained at 37°C in Dulbecco's Modified Eagle's Medium/Ham's Nutrient Mixture F12 (DMEM/F12) (Invitrogen, Carlsbad, CA) supplemented with 10% fetal bovine serum, 250 U/ml penicillin, 250 μg/ml streptomycin, and 2 mM L-glutamine (Invitrogen) in a 5% CO_2-humidified chamber. ST-2 cells, mouse bone marrow stromal cell line, were maintained in Minimal Essential Medium Alpha (Invitrogen) supplemented with 10% fetal bovine serum, 250 U/ml penicillin, 250 μg/ml streptomycin, and 2 mM L-glutamine (Invitrogen) in a 5% CO_2-humidified chamber.

Establishment of Ace-1 Cells Stably Expressing the Human DKK-1 and Yellow Fluorescent Protein-Luciferase (YFP-Luc) Reporter Gene

Ace-1 cells were transfected with 10 μg of pcDNA3.1(+)/human DKK-1 (Ace-1-DKK-1) or empty vector (Ace-1-Vector) under control of the CMV promoter and 10 μl of Lipofectamine 2000 (Invitrogen). Coding sequence of human DKK-1 (accession no. NM_012242; position 155–955) was cloned into pcDNA3.1 vector (Invitrogen). Stably integrated cells were selected using 2,000 μg/ml of G418 (Sigma–Aldrich Co., St. Louis, MO) for 1 month. Ace-1-DKK-1 and Ace-1-Vector stable cells were transduced with the retroviral yellow fluorescent protein-luciferase (YFP-Luc) dual reporter gene and 8 μg/ml polybrene by spin inoculation at 2,700 rpm for 1 hr at 32°C as described previously [23]. The resulting cells were named Ace-1-DKK-1$^{YFP\text{-}Luc}$ and Ace-1-Vector$^{YFP\text{-}Luc}$, respectively. All the experiments were performed with pooled G418 resistant cells in both DKK-1 expressing cells and vector control groups.

DKK-1 ELISA

DKK-1 concentrations were measured using the DuoSet Human DKK1 ELISA Kit as described previously [5] (R&D Systems, Minneapolis, MN, USA). The lowest standard of the assay was 62.5 pg/ml.

Cell Proliferation

Ace-1-Vector$^{YFP\text{-}Luc}$ cells and Ace-1-DKK-1$^{YFP\text{-}Luc}$ were plated in 6-well plates at a density of 5×10^3 cells per well in triplicate and cultured in DMEM/F12 supplemented with 10% fetal bovine serum, 250 U/ml penicillin, 250 μg/ml streptomycin, and 2 mM L-glutamine. The proliferation assay was performed for 8 days.

Total number of viable cells were counted every 2 days using the trypan blue dye exclusion method.

Inoculation of Ace-1 Cells into Nude Mice

Subcutaneous, intracardiac, and intratibial injections of Ace-1-Vector$^{YFP\text{-}Luc}$ cells and Ace-1-DKK-1$^{YFP\text{-}Luc}$ cells were performed in 6-week-old male nu/nu mice (National Cancer Institute, Frederick, MD) under general anesthesia using a 3% isoflurane (Abbott Laboratories, North Chicago, IL)-oxygen mixture. A total of 5×10^5 Ace-1-Vector$^{YFP\text{-}Luc}$ cells or Ace-1-DKK-1$^{YFP\text{-}Luc}$ suspended in 250 μL of sterile Dulbecco's phosphate-buffered solution (PBS) (Invitrogen) were injected subcutaneously (N = 12 per group) over the dorsal scapular area of the mice. Left cardiac ventricular (N = 12 per group) and intratibial (N = 15 per group) injections were performed with 1×10^5 tumor cells suspended in 100 μL of PBS. Mice with subcutaneous, intracardiac, and intratibial injections were sacrificed at 6 weeks, 4 weeks, and 19 days, respectively.

Bioluminescent Imaging

Bioluminescent imaging was completed using the IVIS 100 in vivo imaging system (Caliper Life Sciences, Hopkinton, MA) as previously described [5]. The photon signal intensity was quantified using Living-Image software version 2.50 (Caliper Life Sciences).

Radiography

Radiographic images of mice were obtained immediately after sacrificing using a Faxitron cabinet radiography system LX-60 (Faxitron X-ray Corp., Wheeling, IL) at 30 kVp for 10 sec.

Histopathology

Complete necropsies were performed on mice and tissues were fixed in 10% neutral-buffered formalin at 4°C for 24 hr. Bones were decalcified in 10% EDTA (pH 7.4) for 2 weeks at 4°C and embedded in paraffin, sectioned (5 μm), and stained with hematoxylin and eosin (H&E) or stained for tartrate-resistant acid phosphatase (TRAP)-positive osteoclasts (Sigma–Aldrich, St. Louis, MO) (kit number 386A-1KT) as previously described [5]. Bone histomorphometry was performed using the Image-Pro Plus, *ver* 6.3 software (Media Cybernetics, Silver Spring, MD). Tibial trabecular bone area, new woven bone area (in the metaphysis and diaphysis), cortical endosteal eroded surface, and cortical endosteal surface covered with new woven bone were measured.

Microcomputed Tomography (μCT)

Nineteen days after inoculation of Ace-1 cells, the mice were sacrificed, tibial bones were demuscled, and fixed in 10% neutral-buffered formalin at 4°C for 24 hr. Formalin was replaced with 70% ethyl alcohol and transferred to 1.7 ml microcentrifuge tube for high resolution μCT scanning (Inveon, Siemens Corporation., New York, NY). Tibial bones were scanned at binning 2, 80 kV energy, 500 mA current for a total of 400 projections. Tibial images were reconstructed and analyzed for morphometry using Inveon research workplace software (IRW) (Siemens). Trabecular bone volume in the metaphyseal region and new woven bone volume in the diaphyseal region of tibial bones between the Ace-1-vector and Ace-1-DKK-1 groups were quantified using the IRW software.

Western Blotting

Total protein was extracted from subcutaneous tumors using M-PER reagent (Pierce, Rockford, IL). Approximately 50 μg of protein lysates were separated on 4–12% Tris–glycine SDS–PAGE gels (Invitrogen). Proteins were transferred to a nitrocellulose membrane and probed with primary antibodies for DKK-1 (1:1,000 dilution, R&D Systems), β-catenin (1:1,000, Abcam, Cambridge, MA) and β-actin (1:1,000, Sigma), total c-Jun amino-terminal kinase (JNK) (1:1,000), and phospho-JNK (1:500, Cell Signaling Technology, Inc. Danvers, MA) followed by incubation with horseradish peroxidase-conjugated goat anti-rabbit secondary antibody (1:20,000, Promega, Madison, WI) or goat anti-mouse antibody (1:10,000, Abcam). The signal was detected by chemiluminescent ECL Plus^{TM} western blotting detection reagent (GE Healthcare Bio-Sciences Corp., Piscataway, NJ).

RNA Extraction and ReverseTranscription-Polymerase Chain Reaction (RT-PCR)

Total RNA was extracted from Ace-1 cells using Trizol reagent (Invitrogen). Total RNA (1 μg) was reverse transcribed using the Superscript II First Strand cDNA synthesis kit (Invitrogen) and PCR was performed on the cDNA for the genes DKK-1, Wnt4, Wnt5A, Wnt7, LRP5, LRP6, and beta-2-microglubulin (β2M) using canine-specific primers as shown in Table I.

Collection of Conditioned Medium

Ace-1-Vector$^{YFP\text{-}Luc}$ and Ace-1-DKK-1$^{YFP\text{-}Luc}$ cells were plated in a 6-well plate in triplicate and cultured in DMEM/F12 supplemented with 1% fetal bovine serum for 48 hr to collect conditioned medium. Conditioned medium was stored at −80°C until used.

TABLE I. Dog-Specific Primers Used for RT-PCR Amplification of Expressed Genes

Gene	Forward primer (5′–3′)	Reverse primer (5′–3′)
DKK-1	ATCGAGGAGAGATCGAGGAGA	ATGATCGGAGACAGACCGAG
LRP5	ACATGTACTGGACAGACTGG	AGTCTGTCCAGTACAGAGTG
LRP6	GTACAGAATGTTGTTGTCTCTGG	TTGAACCATCCATTCCAGCA
Wnt4	AACCTGGAGGTGATGGACTC	ACTTCTCCAGCTCCCCGCT
Wnt5A	AACTGTGCCACTTGTATCAGGA	TAGCCGTAGTCGATGTTGTCC
Wnt7	TACCAGTTCCGCTTCGGACG	AGTTGCTCAGGTTACCCTGGCT
β2M	CTTGCTCCTCATCCTCCTC	TGACACGTAGCAGTTCAG

Preostoblast Mineralization Assay

ST-2 murine bone marrow osteoblast precursor cells were grown in minimum essential medium-alpha (Invitrogen) supplemented with 10% FBS, 250 U/ml penicillin, 250 μg/ml streptomycin, and 2 mM L-glutamine. At confluence, the medium was changed and all groups were supplemented with the osteoblast mineralization factors, 100 μM ascorbic acid (Fisher Scientific International, Inc., Fair Lawn, NJ), and 5 mM β-glycerophosphate (MP Biomedicals, Inc., Solon, OH). Treatment groups were treated with 50% conditioned medium from Ace-1-Vector$^{YFP\text{-}Luc}$ and Ace-1-DKK-1$^{YFP\text{-}Luc}$ cells, respectively. Medium was changed every three days and the assay was performed for 21 days. On day 21, mineralization of the ST-2 cells was detected by von Kossa staining. Cells were fixed in 95% ethanol for 10 min and rinsed with distilled water. Cells were treated with 5% silver nitrate (Sigma–Aldrich, Inc., St. Louis, MO) for 20 min and rinsed with distilled water. Cells were treated with 0.5% hydroquinone (Acros Organics, Geel, Belgium) and exposed to ultraviolet light for 5 min. Cells were rinsed with distilled water and treated with 5% sodium thiosulfate (Fisher) for 5 min and rinsed in distilled water and air dried.

Transfections

To investigate the effect of Ace-1 cells on TCF reporter transcriptional activity in murine bone marrow osteoblast precursor cells (ST2), approximately 80–90% confluent ST2 cells in 6-well plates in triplicate were transfected with 1 μg of either wild-type pGL2/TCF/Luc (Top) (Keller lab), mutant pGL2/TCFP2/Luc (FOP) constructs using 5 μL of Lipofectamine 2000 reagent (Invitrogen) for 6 hr. Then medium was removed, washed with PBS and replaced with fresh medium. Either Ace-1-Vector or Ace-1-DKK-1 cells (1×10^4) were added to the ST2 cells transfected with TOP or FOP vector and co-cultured for 48 hr. The plasmid pβgal-Vector (200 ng) was included in each transfection reaction to correct for transfection efficiency. Luciferase activity of ST2 cells was measured with the luciferase assay system (Promega) using 20 μl of lysate. β-Galactosidase activity was measured with the luminescent β-galactosidase detection kit II (BD Biosciences, Palo Alto, CA) and β-galactosidase activity was used to normalize for transfection efficiency. Finally, wild-type TOP luciferase reporter transcriptional activity was normalized with the mutant (FOP) luciferase reporter transcriptional activity.

Statistics

All groups with normally distributed variables, unless stated otherwise, were compared by two-tailed Student's *t*-tests. For nonparametric data with two groups, Mann-Whitney rank sum *t*-tests were performed (Fig. 2). For comparison of multiple groups, one-way ANOVA was used followed by Tukey's post hoc test to perform pair-wise comparisons (Fig. 6) using SigmaPlot software *Ver* 11.0 (Chicago, IL). Results were displayed as means ± standard deviations (SD). Data with P values < 0.05 were considered statistically significant.

RESULTS

Ace-1 Prostate Cancer Cells Expressed Wnt Genes and Their Receptors

Because Wnts play an important role in oncogenesis and osteogenesis, we evaluated the expression of Wnt genes in Ace-1 cells by RT-PCR using dog-specific primers. Ace-1 cells expressed mRNAs for Wnt 4, Wnt 5A, and Wnt 7 (Fig. 1A). Ace-1 cells also expressed DKK-1, LRP 5, and LRP 6 receptors (Fig. 1A). Although Ace-1 cells expressed DKK-1 mRNA, secreted DKK-1 protein was below the level of detection (using the DKK-1 ELISA kit). Ace-1 cells were transfected with human DKK-1 resulting in Ace-1-DKK-1 cells stably expressing human DKK-1. The Ace-1-DKK-1 cells produced approximately 10 ng/ml/10^5 cells of DKK-1 at 72 hr as detected by ELISA (Fig. 1B).

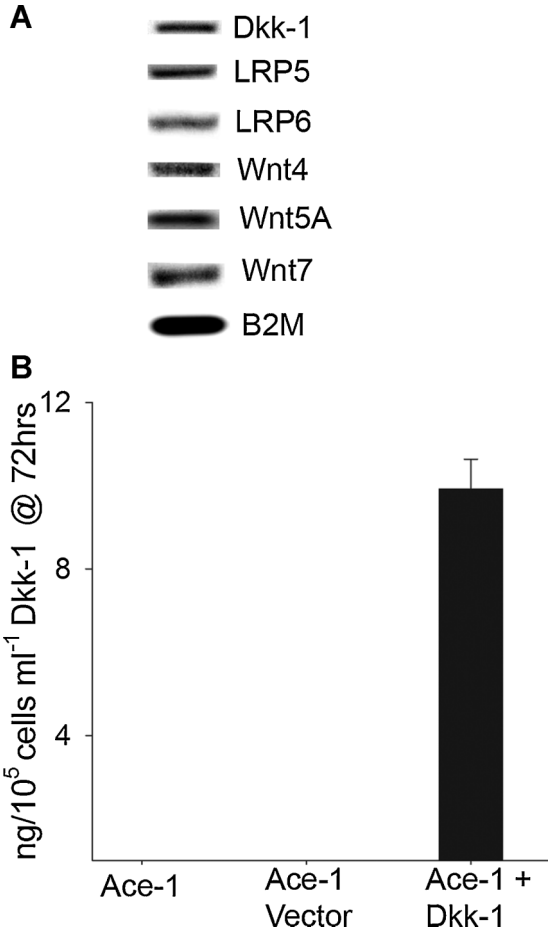

Fig. 1. Expression of Wnt family genes in Ace-1 prostate cancer cells. **A**: Expression of Wnt genes, LRP receptors, and DKK-1 was measured by RT-PCR in Ace-1 cells. **B**: Ace-1 cells were transfected with human DKK-1 and secreted DKK-1 was measured by ELISA at 72 hr.

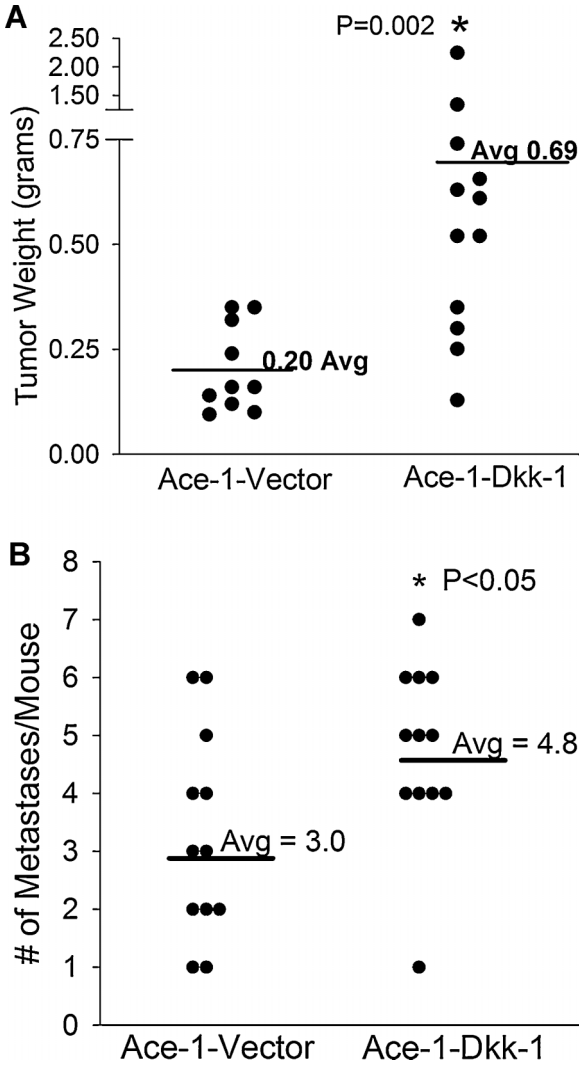

Fig. 2. Effect of DKK-1 on Ace-1 prostate cancer subcutaneous tumor growth and bone metastasis incidence. **A**: Subcutaneous tumor weights from the Ace-1-Vector and Ace-1-DKK-1 groups were measured at 42 days post-injection. $*P = 0.002$ compared to Ace-1-Vector group. **B**: Intracardicac injections were performed with Ace-1-Vector$^{YFP\text{-}Luc}$ or Ace-1-DKK-1$^{YFP\text{-}Luc}$ cells. Incidence of metastatic sites was counted using bioluminescent imaging and number of metastases per animal per group were shown using vertical dot plots. $*P < 0.05$ compared to Ace-1-Vector$^{YFP\text{-}Luc}$.

Effect of DKK-1 on Ace-1 Subcutaneous Growth and Incidence of Bone Metastases

To measure the effect of DKK-1 on Ace-1 tumor growth subcutaneous injections were performed with Ace-1-Vector$^{YFP\text{-}Luc}$ or Ace-1-DKK-1$^{YFP\text{-}Luc}$ cells in athymic mice. After 6 weeks, mice were sacrificed and tumors were weighed. There was a 3.5-fold ($P < 0.002$) increase in tumor weight in Ace-1-DKK-1$^{YFP\text{-}Luc}$ compared to the Ace-1-Vector$^{YFP\text{-}Luc}$ group (Fig. 2A). However, there was no difference in in vitro proliferation between the cell lines (data not shown). To evaluate the effect of DKK-1 on bone metastasis incidence, left ventricular intracardiac injections were performed with Ace-1-Vector$^{YFP\text{-}Luc}$ or Ace-1-DKK-1$^{YFP\text{-}Luc}$ cells and incidence of bone metastases was measured by bioluminescent imaging on days 14, 21, and 28. The Ace-1-DKK-1$^{YFP\text{-}Luc}$ cells had a significantly ($P < 0.05$) greater number of bone metastases compared to Ace-1-Vector$^{YFP\text{-}Luc}$ cells (Fig. 2B).

Role of DKK-1 in Ace-1 Wnt Canonical and Noncanonical Signaling

To confirm the expression of DKK-1 in Ace-1-DKK-1$^{YFP\text{-}Luc}$ tumors, total protein lysates were

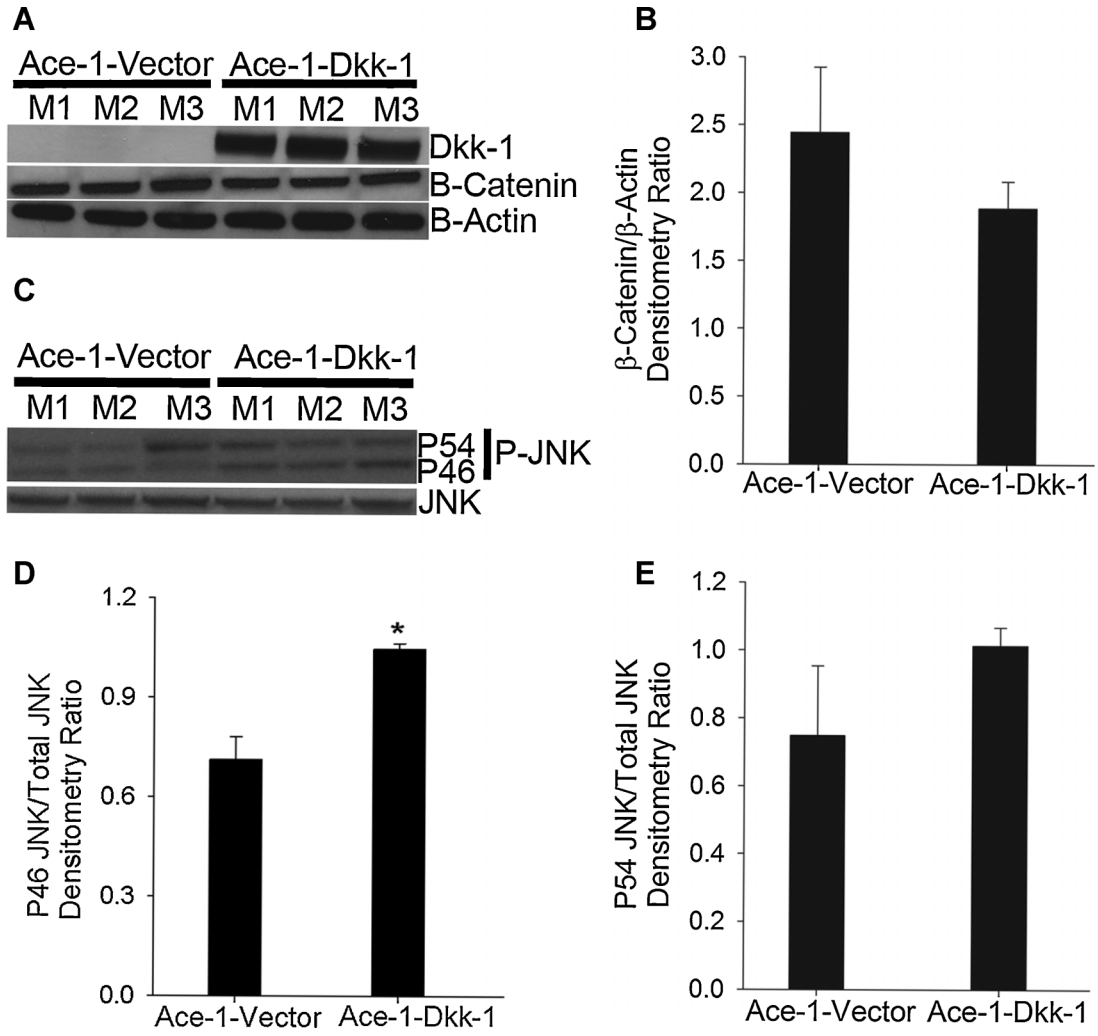

Fig. 3. Measurement of DKK-I autocrine canonical and noncanonical signaling in Ace-I subcutaneous tumors. **A**: Western blotting was performed on total protein lysates isolated from three different subcutaneous tumors from each group for DKK-I, β-catenin, and β-actin. **B**: β-catenin protein expression was analyzed by densitometry and normalized to the loading control, β-actin. **C**: Western blots were performed on total protein lysates from subcutaneous tumors for phospho-JNK and total JNK. **D** and **E**: Densitometric analysis of phospho46 (p46) and phospho54 (P54) JNK isoforms compared to total JNK concentrations. *$P < 0.001$.

extracted and immunoblotted with antibodies to DKK1. As shown in Figure 3A, Ace-1-DKK-1$^{YFP\text{-}Luc}$ tumors had marked DKK-1 protein expression and no DKK-1 was detected in the Ace-1-Vector$^{YFP\text{-}Luc}$ tumors. DKK-1 is shown to act primarily by interacting with LRP5/6 receptors to inhibit Wnt signaling. In order to assess the functional significance of the Wnts in Ace-1-DKK-1$^{YFP\text{-}Luc}$ tumor growth, we measured the expression of β-catenin, which plays an important role in Wnt canonical signaling (Fig. 3A). Interestingly, as shown in Figure 3A and B, there was no significant difference in the levels of β-catenin in the Ace-1-DKK-1$^{YFP\text{-}Luc}$ tumors compared to Ace-1-Vector$^{YFP\text{-}Luc}$ tumors. β-actin was used as a loading control for protein and β-catenin expression was normalized to β-actin in Figure 3B.

Because phosphorylation of JNK is one of the functional consequences of Wnt noncanonical signaling, we measured phosphorylated JNK in Ace-1-DKK-1$^{YFP\text{-}Luc}$ tumors compared to Ace-1-Vector$^{YFP\text{-}Luc}$ tumors. As shown in Figure 3C and D, there was a significantly ($P < 0.001$) greater level of phospho46 (P46) JNK isoform in the Ace-1-DKK-1$^{YFP\text{-}Luc}$ tumors compared to Ace-1-Vector$^{YFP\text{-}Luc}$. Whereas the levels of phospho54 (P54) isoform were slightly higher in Ace-1-DKK-1$^{YFP\text{-}Luc}$ tumors compared to Ace-1-Vector$^{YFP\text{-}Luc}$ tumors, the difference was not significant (Fig. 3C

and E). Densitometry ratios in Figure 3D and E were normalized to total JNK protein expression.

Effect of Ace-1 Conditioned Medium on In Vitro Mineralization of Mouse Preosteoblast ST-2 Cells

Ace-1 Cells Conditioned Medium Did Not Induce Mineralization of Mouse ST-2 Cells In Vitro (Data Not Shown).

Radiographic Evaluation of DKK-1 on Ace-1 Osteoblastic Metastases

To analyze the effect of DKK-1 on the Ace-1-induced osteoblastic metastases, radiographs of all tibial bones were made on day 19. In the Ace-1 Vector group, there was increased radio-opacity in the medullary region of the diaphysis compared to the contralateral, uninjected tibia (Fig. 4). In contrast, DKK-1 overexpressing intramedullary tumors had marked loss of cortical and trabecular bone in the metaphyses and diaphyses of the tibias (Fig. 4) compared to the Ace-1-vector group. This suggested that DKK-1 inhibited the Ace-1-induced new bone formation in the intratibial model of bone metastases.

Histopathologic Evaluation of Intratibial Osteoblastic Metastases

To investigate the effect of DKK-1 on the osteoblastic phenotype of bone metastases, H&E-stained sections of the tibias that were injected with Ace-1 cells from both groups were examined. Intratibial injections of Ace-1 cells resulted in growth of tumor cells from the growth plate to the diaphyseal regions replacing most of the bone marrow. As evidence of the mixed osteoblastic/osteolytic nature of Ace-1 cells, mild trabecular bone lysis was present in the metaphyses of the vector group. Additionally, the Ace-1 vector group demonstrated marked tumor-induced new woven bone formation along the endosteal surface of the tibia and in the medullary region of diaphysis resulting in an osteoblastic phenotype of bone metastasis (Fig. 5A). In contrast, in the DKK-1 overexpressing group, marked lysis of trabecular bone and tumor-induced resorption of the cortical endosteum was present demonstrating that Ace-1 cells overexpressing DKK-1 significantly inhibited the Ace-1-induced osteoblastic phenotype (Fig. 5A). Histomorphometric analysis showed that the trabecular bone volume in tibias with DKK-1 overexpressing Ace-1 cells was significantly decreased (approximately four-fold) compared to the vector group (Fig. 5B). Also, the new woven bone surface area was approximately three-fold reduced in the Ace-1-DKK1 group compared to Ace-1-Vector group (Fig. 5C).

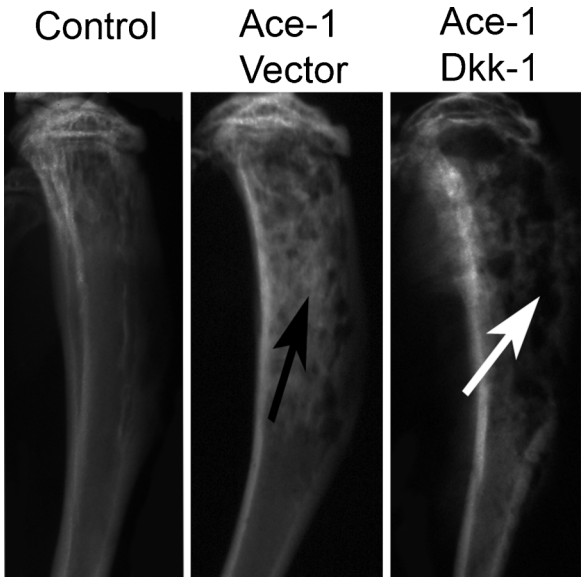

Fig. 4. Radiographic analysis of DKK-1 on Ace-1 intratibial bone metastases. Radiographs were taken 19 days after the intratibial inoculation of Ace-1-Vector$^{YFP\text{-}Luc}$ or Ace-1-DKK-1$^{YFP\text{-}Luc}$ cells. Tibias in the Ace-1-Vector$^{YFP\text{-}Luc}$ group had increased radio-opacity in the diaphyseal region (black arrow) compared to the control bone that did not receive any tumor cells. Tibias in the Ace-1-DKK-1$^{YFP\text{-}Luc}$ group had cortical and trabecular bone lysis in the metaphyseal and diaphyseal regions (white arrow).

DKK-1 Decreased Tibial Endosteal Eroded Surface and Decreased New Woven Bone Formation

To investigate whether DKK-1 altered Ace-1-induced new woven bone surface and resorption surface along the tumor-tibial cortical endosteal interface, we measured the length of tibial cortical endosteal surface covered by new woven bone and eroded surfaces. Ace-1 cells overexpressing DKK-1 significantly increased the tibial endosteal eroded surface by two-fold compared to Ace-1-Vector group (Table IIA). In addition, the DKK-1 group had markedly decreased new woven bone along (four-fold) the endosteal surface compared to the vector group (Table IIA).

Microcomputed Tomographic Evaluation of DKK-1 on Ace-1 Tibial Metastases

Tibias were scanned by microcomputed tomography after fixing in neutral-buffered formalin for 24 hr. The effect of DKK-1 on Ace-1-induced new woven bone volume was measured using IRW software. Analysis of the μCT images showed that DKK-1 decreased trabecular bone volume approximately six-fold (Table IIB) and new woven bone by five-fold (Table IIB) compared to the Ace-1-vector group.

Role of DKK-1 on Paracrine Canonical Pathway in Mouse Preosteoblast ST2 Cells

Since DKK-1 overexpression markedly inhibited the Ace-1-induced osteoblastic phenotype of bone

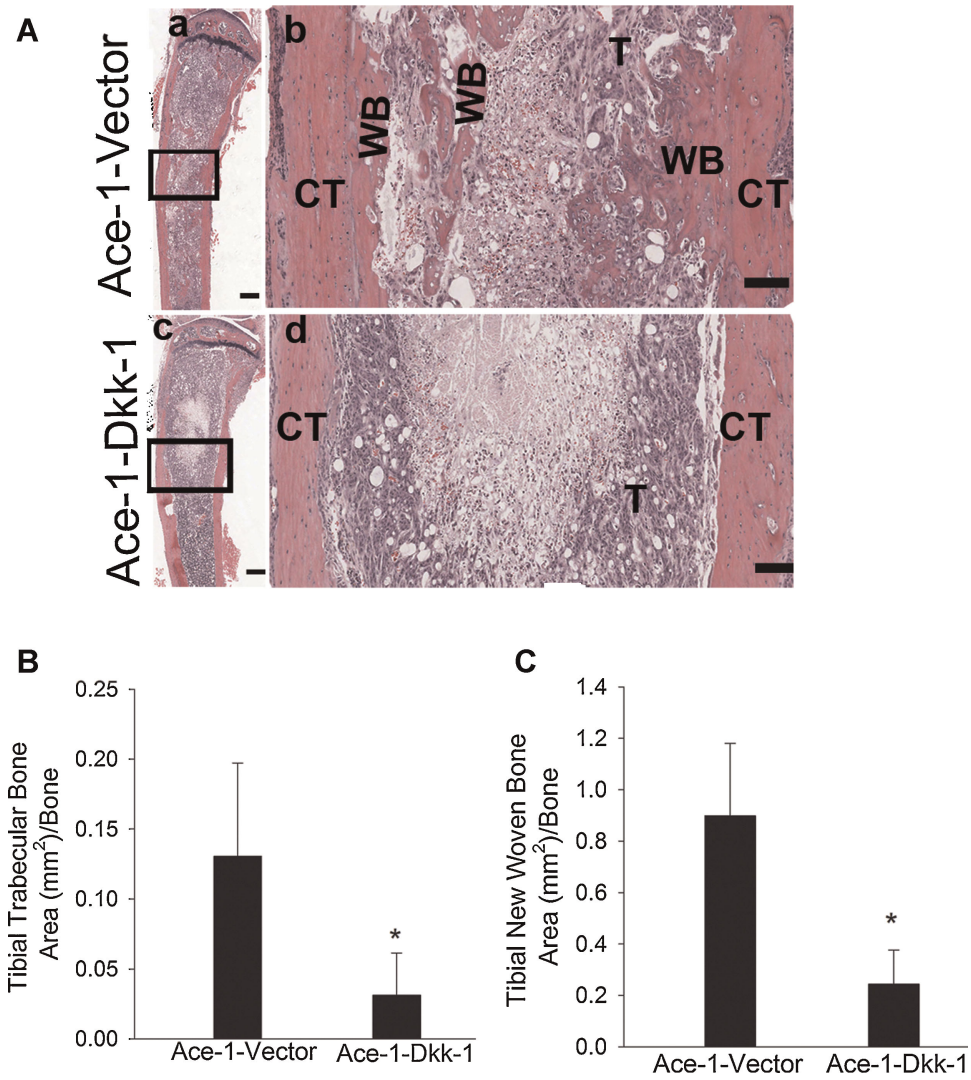

Fig. 5. Histopathologic evaluation of intratibial bone metastases 19 days after intratibial inoculation of Ace-1-Vector$^{YFP\text{-}Luc}$ or Ace-1-DKK-1$^{YFP\text{-}Luc}$ cells. **A**: H&E-stained sections of tibias demonstrated that Ace-1 tumors (T) extending from the growth plate to the diaphyseal region in both groups. In the Ace-1-Vector$^{YFP\text{-}Luc}$ group (a and b) new woven bone (WB) was present along the tumor and endosteal surfaces of the cortex (CT) in the tibial diaphyseal region. In the Ace-1-DKK-1$^{YFP\text{-}Luc}$ group (c and d) new woven bone was absent. *Bar*, a and c = 500 μm, b and d = 100 μm. Histomorphometric analysis showed that DKK1 significantly decreased the trabecular bone (**B**) in the metaphyseal region and new woven bone (**C**) in the tibia compared to the vector group. *$P < 0.001$.

TABLE II. Histomorphometric Quantification of Effect of DKK-1 on Ace-1 Tibial Bone Metastasis

Bone histomorphometry parameter	Ace-1-Vector	Ace-1-DKK-1
A: Histopathologic analysis		
Cortical endosteal eroded surface/total cortical endosteal surface	0.37 ± 0.11	0.74 ± 0.03*
Cortical endosteal surface with new bone/total cortical endosteal surface	0.42 ± 0.14	0.09 ± 0.07*
B: Micro-CT analysis		
Tibial trabecular volume (mm^3)/bone	1.19 ± 0.83	0.19 ± 0.1*
Tibial woven bone volume (mm^3)/bone	2.58 ± 0.6	0.42 ± 0.37*

*$P < 0.001$ compared to Ace-1-Vector.

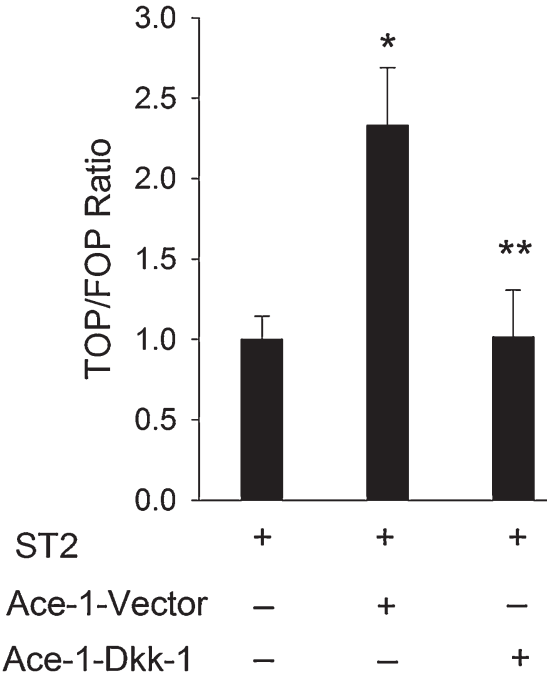

Fig. 6. Effect of Ace-1 cells on in vitro paracrine canonical TCF luciferase reporter transcriptional activity of murine bone marrow precursor osteoblast cells (ST2). Co-culture of ST2 cells and Ace-1-Vector cells increased TCF reporter activity in ST2 cells compared to ST2 cells alone. *$P < 0.003$. Ace-1-DKK-1 cells co-cultured with ST2 cells decreased the ST2 TCF reporter activity compared to vector group ST2 TCF activity. **$P < 0.003$.

metastasis, the effect of DKK-1 on canonical signaling in mouse bone marrow osteoblast precursor cells (ST2) was tested. In the Wnt canonical pathway, β-catenin binds to TCF and activates it for further transcriptional targeting of the Wnt-mediated pathway. Since TCF activity plays an important role in the canonical Wnt pathway, we measured the TCF activity in ST2 cells as an indicator of canonical Wnt signaling. Co-culture of ST2 and Ace-1-Vector cells resulted in a significant increase in the canonical TCF reporter transcriptional activity in ST2 cells. However, co-culture of ST2 cells with Ace-1-DKK-1 cells inhibited the Ace-1-induced TCF activity in ST2 cells (Fig. 6). This indicated that Ace-1 cells induced osteoblast activity through canonical Wnt signaling and this pathway was inhibited by DKK-1 in osteoblasts.

DISCUSSION

In the present study we have shown that Ace-1 prostate cancer cells express Wnts and Wnt receptors LRP5 and LRP6. Overexpression of DKK-1 in Ace-1 cells resulted in increased subcutaneous tumor growth and incidence of bone metastasis, but significantly decreased the osteoblastic phenotype of bone metastases.

DKK-1 has been shown to increase cell proliferation and tumor growth in myeloma and HeLa cells [2,3]. Consistent with published data, DKK-1 overexpression resulted in increased growth of subcutaneous tumors in mice. Overexpression of DKK-1 also increased the incidence of bone metastases following intracardiac injection of Ace-1 cells. DKK-1 was significantly increased in breast cancer patients with bone metastases compared to patients with nonbone metastases and healthy women [21]. Therefore, the results of this investigation indicate that DKK-1 may contribute to the increased incidence of bone metastases as reported with breast cancer.

Wnts act through both canonical and noncanonical signaling pathways [14]. In the canonical pathway, Wnts function by binding to low density LRP and frizzled receptors on the target cells to mediate Wnt signaling through β-catenin [15]. In our study there was no upregulation of β-catenin in the Ace-1-DKK-1 cells compared to the Ace-1-Vector-1 cells indicating that the signaling did not occur using the canonical pathway. In human prostate cancer, dysregulation of factors involved in the canonical Wnt pathway such as APC gene mutations [24], downregulation or absence of GSK3β expression [25], axin gene mutations [26], and β-catenin mutations [27] at phosphorylation sites important for ubiquitination and further degradation were reported. In addition, mutated forms of LRP5 or LRP6 receptors were also shown to elicit constitutive canonical Wnt signaling [28,29]. Dysregulation of any of the pathway constituents could be the cause for the absence of β-catenin induction in the Ace-1 cells [30]. Since DKK-1 overexpression did not have a significant effect on the canonical pathway in Ace-1 cells, constitutive activation of canonical Wnt signaling must be considered.

Although the Wnt noncanonical pathway is not well understood, it has been shown that JNK, Rho, and Rock pathways are involved [15]. DKK-1 increased JNK activity and its phosphorylation leading to enhanced survivability of lymphoma cells [31,32]. Endo et al. [33] showed that DKK-1 increased the phosphorylation of JNK in the noncanonical pathway through the frizzled receptor. We investigated noncanonical signaling in Ace-1-DKK-1 cells by examining the phosphorylation of JNK. Western blots showed that the p46 isoform was markedly increased although the p54 isoform was only mildly increased. Yaccoby et al. [34] reported that inhibition of DKK-1 in myeloma using an anti-human DKK-1-neutralizing antibody significantly decreased myeloma growth and osteolysis. Therefore, DKK-1 may be contributing to the to the increased Ace-1 tumor growth seen in this study via the noncanonical pathway by upregulating phosphorylation of JNK. Since there was no difference in in vitro proliferation between the

cell lines, we speculate that the increased in vivo subcutaneous growth was due to a paracrine interaction with the tumor microenvironment.

Moreover, DKK-1 increased the incidence of Ace-1 bone metastases following intracardiac inoculation of cells. It is possible that increased survivability of Ace-1 cells through elevated p46 JNK levels might be contributing to the establishment of a greater number of bone metastases.

Secretion of Wnt 7B by prostate cancer was reported to induce osteogenic activity through the canonical signaling pathway mediated by the LRP5 receptor in immunodeficient mice and DKK-1 blocked the osteogenic activity [35]. Therefore, based on the previous data on DKK-1 mechanism of action on osteoblasts, in this model, we speculated that DKK-1 inhibited the Wnt-induced osteoblastic activity through the canonical pathway. The data from the TCF reporter transcriptional assay showed that Ace-1 cells induced activation of Wnt/TCF canonical signaling in ST2 cells. This demonstrated that Ace-1 cells likely induced osteoblastic activity through canonical signaling. Importantly, Ace-1 cells overexpressing DKK-1 inhibited Ace-1-induced canonical TCF activity in ST2 precursor osteoblasts showed that DKK-1 inhibited Ace-1-induced osteoblast activity through a paracrine mechanism. This was supported by the in vivo data that DKK-1 inhibited Ace-1-induced intratibial woven bone formation at the site of tumor cell inoculation. The in vitro mineralization assay showed that Ace-1 cell conditioned medium was not sufficient to induce differentiation of preosteoblats. However, the induction of new bone formation by Ace-1 cells in vivo suggests that cellular and paracrine interactions in the bone microenvironment are necessary for Ace-1 cells to induce new bone formation. Disruption of Ace-1 induced new bone formation by DKK-1 overexpression demonstrated that Wnt signaling was important for Ace-1-induced new bone formation in vivo.

Radiographic and histopathologic evaluation of tibias with Ace-1 cells showed that DKK-1 overexpressing cells significantly decreased new bone formation induced by Ace-1 cells as demonstrated by a marked decrease in trabecular and new woven bone area. Micro-CT imaging also demonstrated a marked decrease in trabecular and new woven bone volume. DKK-1 increased endosteal eroded surface in the tibias and decreased endosteal new woven bone surface. This demonstrated that DKK-1 secreted by Ace-1 cells not only inhibited osteoblast activity but also indirectly led to increased osteoclast activity. This data supports the previously reported findings that DKK-1 plays a significant role in determining the phenotype of human prostate cancer bone metastases [19].

Although DKK-1 has no direct effect on osteoclastogenesis, it has been reported that DKK-1 inhibited the secretion of osteoprotegerin (OPG) and induced RANKL secretion from osteoblasts resulting in an increased RANKL:OPG ratio, which has been shown to be important for enhanced osteoclastogenesis [36]. In the current study, it is possible that DKK-1 inhibited the Ace-1-induced osteoblastic phenotype of bone metastases by directly inhibiting osteoblasts via the canonical pathway and by stimulating osteoclastogenesis indirectly through increasing the RANKL:OPG ratio.

Although DKK-1 significantly decreased Ace-1-induced new bone formation in osteoblastic metastases, its unexpected role in the increased prostate cancer growth and bone metastases incidence further necessitates investigations to clearly understand the role of Wnt canonical and noncanonical pathways in the pathogenesis of prostate cancer.

ACKNOWLEDGMENTS

We thank Tim Vojt for help with preparation of the figures and Wessel Dirksen for help with laboratory work and Alan Fletcher for help with histology work.

REFERENCES

1. Coleman RE. Skeletal complications of malignancy. Cancer 1997;80:1588–1594.
2. Crawford ED. Skeletal complications in men with prostate cancer: Effects on quality-of-life outcomes throughout the continuum of care. Eur Urol Suppl 2004;3:10–15.
3. Roodman GD. Mechanisms of bone metastasis. New England J Med 2004;350:1655–1664.
4. Mundy GR. Metastasis to bone: Causes, consequences and therapeutic opportunities. Nat Rev Cancer 2002;2:584–593.
5. Thudi NK, Martin CK, Nadella MVP, Fernandez SA, Werbeck JL, Pinzone JJ, Rosol TJ. Zoledronic acid decreased osteolysis but not bone metastasis in a nude mouse model of canine prostate cancer with mixed bone lesions. Prostate 2008;68:1116–1125.
6. Liao J, Li X, Koh AJ, Berry JE, Thudi N, Rosol TJ, Pienta KJ, McCauley LK. Tumor expressed PTHrP facilitates prostate cancer-induced osteoblastic lesions. Int J Cancer 2008;123:2267–2278.
7. Mundy GR. Endothelin-1 and osteoblastic metastasis. Proc Natl Acad Sci 2003;100:10588–10589.
8. Lu W, Tinsley HN, Keeton A, Qu Z, Piazza GA, Li Y. Suppression of Wnt/β-catenin signaling inhibits prostate cancer cell proliferation. Eur J Pharmacol 2009;602:8–14.
9. Logan CY, Nusse R. The Wnt signaling pathway in development and disease. Annu Rev Cell Dev Biol 2004;20:781–810.
10. Polakis P. Wnt signaling and cancer. Genes Dev 2000;14:1837–1851.
11. Katoh M, Kirikoshi H, Terasaki H, Shiokawa K. WNT2B2 mRNA, up-regulated in primary gastric cancer, is a positive regulator of the WNT–β-catenin–TCF signaling pathway. Biochem Biophys Res Commun 2001;289:1093–1098.
12. Saitoh T, Mine T, Katoh M. Up-regulation of WNT 8 B mRNA in human gastric cancer. Int J Oncol 2002;20:343–348.

13. Chen G, Shukeir N, Potti A, Sircar K, Aprikian A, Goltzman D, Rabbani SA. Up-regulation of Wnt-1 and β-catenin production in patients with advanced metastatic prostate carcinoma. Cancer 2004;101:1345–1356.
14. Liu G, Bafico A, Aaronson SA. The mechanism of endogenous receptor activation functionally distinguishes prototype canonical and noncanonical Wnts. Mol Cell Biol 2005;25:3475–3482.
15. Pinzone JJ, Hall BM, Thudi NK, Vonau M, Qiang YW, Rosol TJ, Shaughnessy JD Jr. The role of Dickkopf-1 in bone development, homeostasis, and disease. Blood 2009;113:517–525.
16. Van de Wetering M, Cavallo R, Dooijes D, Van Beest M, Van Es J, Loureiro J, Ypma A, Hursh D, Jones T, Bejsovec A, Peifer M, Mortin M, Clevers H. Armadillo coactivates transcription driven by the product of the drosophila segment polarity gene dTCF. Cell 1997;88:789–799.
17. Barker N, Clevers H. Mining the Wnt pathway for cancer therapeutics. Nat Rev Drug Discovery 2006;5:997–1014.
18. Day TF, Guo X, Garrett-Beal L, Yang Y. Wnt/β-catenin signaling in mesenchymal progenitors controls osteoblast and chondrocyte differentiation during vertebrate skeletogenesis. Dev Cell 2005;8:739–750.
19. Hall CL, Bafico A, Dai J, Aaronson SA, Keller ET. Prostate cancer cells promote osteoblastic bone metastases through Wnts. Cancer Res 2005;65:7554–7560.
20. Hall CL, Kang S, MacDougald OA, Keller ET. Role of Wnts in prostate cancer bone metastases. J Cell Biochem 2006;97:661–667.
21. Voorzanger-Rousselot N, Goehrig D, Journe F, Doriath V, Body J, Clezardin P, Garnero P. Increased Dickkopf-1 expression in breast cancer bone metastases. Br J Cancer 2007;97:964–970.
22. LeRoy BE, Thudi NK, Nadella MVP, Toribio RE, Tannehill-Gregg SH, van Bokhoven A, Davis D, Corn S, Rosol TJ. New bone formation and osteolysis by a metastatic, highly invasive canine prostate carcinoma xenograft. The Prostate 2006;66:1213–1222.
23. Nadella MV, Kisseberth WC, Nadella KS, Thudi NK, Thamm DH, McNiel EA, Yilmaz A, Boris-Lawrie K, Rosol TJ. NOD/SCID mouse model of canine t-cell lymphoma with humoral hypercalcaemia of malignancy: Cytokine gene expression profiling and in vivo bioluminescent imaging. Vet Comp Oncol 2008;6:39–54.
24. Watanabe M, Kakiuchi H, Kato H, Shiraishi T, Yatani R, Sugimura T, Nagao M. APC gene mutations in human prostate cancer. Jpn J Clin Oncol 1996;26:77.
25. Davies G, Jiang WG, Mason MD. Cell-cell adhesion molecules and signaling intermediates and their role in the invasive potential of prostate cancer cells. J Urol 2000;163:985–992.
26. Yardy GW, Bicknell DC, Wilding JL, Bartlett S, Liu Y, Winney B, Turner GDH, Brewster SF, Bodmer WF. Mutations in the AXIN1 gene in advanced prostate cancer. Eur Urol 2009;56:486–494.
27. Voeller HJ. Beta-catenin mutations in human prostate cancer. Cancer Res 1998;58:2520–2523.
28. Mao B, Wu W, Li Y, Hoppe D, Stannek P, Glinka A, Niehrs C. LDL-receptor-related Protein 6 is a receptor for Dickkopf proteins. Nature 2001;411:321–324.
29. Mao J, Wang J, Liu B, Pan W, Farr GH, Flynn C, Yuan H, Takada S, Kimelman D, Li L. Low-density lipoprotein receptor-related Protein-5 binds to axin and regulates the canonical Wnt signaling pathway. Mol Cell 2001;7:801–809.
30. Bafico A, Liu G, Goldin L, Harris V, Aaronson SA. An autocrine mechanism for constitutive Wnt pathway activation in human cancer cells. Cancer Cell 2004;6:497–506.
31. Pandur P, Läsche M, Eisenberg LM, Kühl M, WNT-11 activation of a non-canonical wnt signaling pathway is required for cardiogenesis. Nature 2002;418:636–641.
32. Gururajan M, Chui R, Karuppannan AK, Ke J, Jennings CD, Bondada S. C-Jun N-terminal kinase (JNK) is required for survival and proliferation of B-lymphoma cells. Blood 2005;106:1382–1391.
33. Endo Y, Beauchamp E, Woods D, Taylor WG, Toretsky JA, Üren A, Rubin JS. Wnt-3a and Dickkopf-1 stimulate neurite outgrowth in Ewing tumor cells via a Frizzled3-and c-Jun N-terminal kinase-dependent mechanism. Mol Cell Biol 2008;28:2368–2379.
34. Yaccoby S, Ling W, Zhan F, Walker R, Barlogie B, Shaughnessy JD Jr. Antibody-based inhibition of DKK1 suppresses tumor-induced bone resorption and multiple myeloma growth in vivo. Blood 2007;109:2106–2111.
35. Yang M, Jiang P, Sun FX, Hasegawa S, Baranov E, Chishima T, Shimada H, Moossa A, Hoffman RM. A fluorescent orthotopic bone metastasis model of human prostate cancer 1. Cancer Res 1999;59:781–786.
36. Qiang YW, Chen Y, Stephens O, Brown N, Chen B, Epstein J, Barlogie B, Shaughnessy JD Jr. Myeloma-derived Dickkopf-1 disrupts Wnt-regulated osteoprotegerin and RANKL production by osteoblasts: A potential mechanism underlying osteolytic bone lesions in multiple myeloma. Blood 2008;112:196–207.